THE JOURNAL OF PHYSICAL CHEMISTRY C

Article

Cite This: J. Phys. Chem. C 2019, 123, 8421−8428

pubs.acs.org/JPCC

Surface Segregation in CuNi Nanoparticle Catalysts During CO_2 Hydrogenation: The Role of CO in the Reactant Mixture

Ioannis Zegkinoglou,[†] Lukas Pielsticker,[†] Zhong-Kang Han,[‡] Nuria J. Divins,[†] David Kordus,[†] Yen-Ting Chen,[†] Carlos Escudero,[§] Virginia Pérez-Dieste,[§] Beien Zhu,[‡] Yi Gao,[‡] and Beatriz Roldan Cuenya*[,∥]

[†]Department of Physics, Ruhr University Bochum, 44780 Bochum, Germany

[‡]Division of Interfacial Water and Key Laboratory of Interfacial Physics and Technology, Shanghai Institute of Applied Physics, Chinese Academy of Sciences, Shanghai 201800, China

[§]ALBA Synchrotron Light Source, Carrer de la Llum 2-26, Cerdanyola del Vallès, 08290 Barcelona, Spain

[∥]Department of Interface Science, Fritz-Haber Institute of the Max Planck Society, Berlin 14195, Germany

Supporting Information

ABSTRACT: Surface segregation and restructuring in size-selected CuNi nanoparticles were investigated via near-ambient pressure X-ray photoelectron spectroscopy (NAP-XPS) at various temperatures in different gas environments. Particularly in focus were structural and morphological changes occurring under CO_2 hydrogenation conditions in the presence of carbon monoxide (CO) in the reactant gas mixture. Nickel surface segregation was observed when only CO was present as adsorbate. The segregation trend is inverted in a reaction gas mixture consisting of CO_2, H_2, and CO, resulting in an increase of copper concentration on the surface. Density functional theory calculations attributed the inversion of the segregation trend to the formation of a stable intermediate on the nanocatalyst surface (CH_3O) in the CO-containing reactant mixture, which modifies the nickel segregation energy, thus driving copper to the surface. The promoting role of CO for the synthesis of methanol was demonstrated by catalytic characterization measurements of silica-supported CuNi NPs in a fixed-bed reactor, revealing high methanol selectivity (over 85%) at moderate pressures (20 bar). The results underline the important role of intermediate reaction species in determining the surface composition of bimetallic nanocatalysts and help understand the effect of CO cofeed on the properties of CO_2 hydrogenation catalysts.

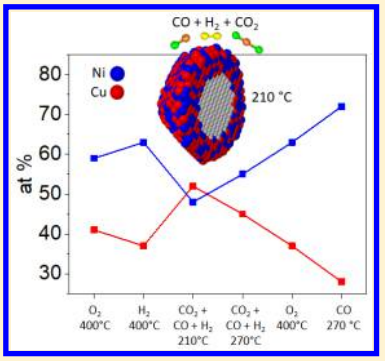

INTRODUCTION

Methanol is industrially produced from the conversion of a synthesis gas mixture consisting of CO, CO_2, and H_2 over $Cu/ZnO/Al_2O_3$ catalysts at moderate temperatures (230−280 °C) and high pressures (50−120 bar). Cu(211) step edges associated with bulk defects, such as stacking faults and twin boundaries terminating at the surface, in combination with nearby Zn atoms acting as adsorption sites for oxygen-bound intermediates, have been shown to be catalytically active in this system.[1] Despite its wide use, the $Cu/ZnO/Al_2O_3$ catalytic system is not free of drawbacks, including low stability due to sintering and the need for high pressures (at least 50 bar). Several studies have shown that doping of Cu catalysts with Ni drastically increases the rate of methanol production from CO_2 + CO + H_2 mixtures,[2−7] whereas such a promoting effect is not observed in reactant mixtures only consisting of CO_2 and H_2.[2] Although ^{14}C-labeling experiments have demonstrated that CO_2 is the main source of carbon for methanol synthesis over Cu in CO_2 + CO + H_2,[8,9] the presence of Ni on the surface of the catalyst is believed to be beneficial, possibly because of the stabilization of CO species, which are then hydrogenated to methanol.[5] It has been suggested that the role of CO in the reactant mixture is solely that of a promoter, inducing surface segregation of Ni, to which CO can then bind.[2,10] While *in situ* infrared spectroscopic studies of CuNi catalysts performed in pure CO have indeed indicated surface segregation of Ni in the exclusive presence of CO,[11] such information has not been reported to date for the catalytic reaction conditions.

Here we report the results of a phase segregation study of CuNi bimetallic nanoparticles (NPs) supported on $SiO_2/Si(111)$ under CO_2 hydrogenation conditions in a gas mixture consisting of CO_2 + CO + H_2. Using near-ambient pressure X-ray photoelectron spectroscopy (NAP-XPS), we observed Ni surface segregation in pure CO, but Cu segregation in the CO_2 + CO + H_2 reactant mixture. Density functional theory (DFT) calculations indicate that the formation of a stable intermediate species (CH_3O) is responsible for the inversion of the segregation trend. These results show that the role of CO in

Special Issue: Hans-Joachim Freund and Joachim Sauer Festschrift

Received: October 10, 2018
Revised: January 9, 2019
Published: January 15, 2019

the reactant mixture needs to be reconsidered and that intermediate reaction products might be key in determining the structure and surface composition of bimetallic catalysts and their catalytic behavior through surface segregation phenomena. Finally, we demonstrate that our CuNi NPs supported on SiO_2 are promising methanol synthesis catalysts due to their high selectivity (>85%) at moderate pressure (20 bar).

EXPERIMENTAL SECTION

Size-selected bimetallic $Cu_{0.5}Ni_{0.5}$ NPs with an average diameter of 5 nm were synthesized via inverse micelle encapsulation in a toluene solution using poly(styrene)-*block*-poly(2-vinylpyridine) (PS-P2VP) diblock copolymers (PS:P2VP ratio of 48500:70000, Polymer Source, Inc.) for the formation of the micellar cages, and copper(II) nitrate hexahydrate ($Cu(NO_3)_2{\cdot}6H_2O$) and nickel(II) nitrate trihydrate ($Ni(NO_3)_2{\cdot}3\ H_2O$) as metal salts. Details of the synthesis procedure have been reported elsewhere.[12] The particles were deposited on SiO_2/Si(111) substrates via dip-coating (at a speed of 5 cm/min), and the polymeric ligands were subsequently removed by an O_2 plasma treatment (SPI Plasma Prep III Plasma Etcher, 20 min, 20 W, 0.5 mbar).

In order to test the catalytic reactivity of the CuNi NPs under realistic reaction conditions, powder catalyst samples consisting of NPs from the same synthesis solution as above, but supported on nanocrystalline silica (12 nm, Strem Chemicals, Inc., 5% nominal weight loading), were prepared by incipient wetness impregnation and subsequent calcination. Thermogravimetric analysis (TGA) in synthetic air (20% O_2, 80% N_2) was performed in a TGA 5500 setup (TA Instruments) with a flow rate of 25 mL/min and a temperature ramp of 2 °C/min up to 700 °C (see Figure S1 in the Supporting Information, SI). According to these results, the catalyst was calcined in synthetic air with a flow rate of 50 mL/min in a furnace oven (Heraeus ROF 4/50) at 400 °C for 4 h to remove the polymeric carbon from the inverse micelle encapsulation synthesis. The actual metal loading of the SiO_2-supported catalysts was determined by inductively coupled plasma optical emission spectrometry (ICP-OES). The results of the ICP-OES measurements are shown in Table S1 in the SI, where additional details on the characterization of the catalyst samples are also provided.

The morphology of the SiO_2/Si(111)-supported NP samples was investigated with atomic force microscopy (AFM) in the initial, as-prepared state (after the *ex situ* O_2 plasma treatment) and after the NAP-XPS studies. The AFM images were acquired in tapping mode (Bruker MultiMode 8). The size distribution of the NPs was determined using the open-source software Gwyddion, based on the particle heights extracted from the AFM images. The morphology of the silica-supported powder catalyst samples was investigated by scanning transmission electron microscopy (STEM) and energy-dispersive X-ray spectroscopy (EDS) (JEM-2800, JEOL), both before and after the catalytic reaction.

NAP-XPS studies of the SiO_2/Si(111)-supported NPs were performed at the beamline CIRCE of the ALBA synchrotron in Barcelona (Spain).[13] In order to obtain depth profile information on the elemental composition of the NPs, Cu 2p and Ni 2p spectra were acquired at two different photon energies: at 1160 eV, where the inelastic mean free path (IMFP) of the photoelectrons in Cu and Ni is approximately 0.6 nm, and at 1540 eV, where the IMFP is approximately 1.1 nm. Detailed values for the IMFPs are given in Table S2 (SI). Measurements were performed consecutively in O_2 (0.4 mbar, 400 °C); in H_2 (0.4 mbar, 400 °C); in a reaction mixture consisting of CO (vol 11.5%), CO_2 (4.5%), and H_2 (84%) (total pressure: 0.48 mbar; 210 and 270 °C); again in O_2 (0.4 mbar, 400 °C); and in pure CO (0.4 mbar, 270 °C). The heating ramp rate was 20 °C/min and the duration of the measurements about 3 h per temperature point. During the initial annealing in O_2, all adventitious carbon species (due to sample transfer in air) are removed from the sample surface prior to the acquisition of the spectra, as confirmed by high-resolution C 1s scans (see Figure S2, Supporting Information). After each annealing step, the sample was cooled down in the gas, the chamber was evacuated, and the new gas (or gas mixture) was introduced at room temperature. The energy calibration in all XPS spectra was performed using the elemental Si $2p_{3/2}$ peak of the SiO_2/Si support at a binding energy of 99.4 eV as reference. The Cu $2p_{3/2}$ and Ni $2p_{3/2}$ regions were fitted with Gaussian−Lorentzian line shapes (ratio 0.3) and a linear background. For details of the fitting procedure, the reader is referred to the SI, as well as to ref 14.

In order to extract the segregation energies, spin-polarized DFT calculations were performed using the Perdew−Burke−Ernzerhof (PBE) generalized gradient approximation (GGA) implemented in the VASP code.[15,16] The valence electronic states were expanded in the basis of plane waves with the core−valence interaction represented using the projector augmented wave (PAW) approach and a cutoff of 400 eV.[17] For the calculation of the adsorption energies of the various gas molecules on the surface of the catalyst, the lateral interactions between the molecules were taken into consideration. The compounds which are more stable and more strongly adsorbed on the surface are those which mostly affect the surface segregation trend. Further information on the calculations is given in the SI.

The catalytic activity measurements of the SiO_2-supported powder catalyst were performed in a stainless steel fixed-bed flow reactor with inner glass coating. A 60 mg portion of the catalyst was mixed with 240 mg of SiC powder (46 grit, Alfa Aesar) and loaded between two quartz wool plugs. The catalyst was reduced in a H_2 + He mixture (vol 20:80) at 400 °C for 1.5 h and a flow rate of 50 mL/min. Afterward, the sample was cooled down to 210 °C, and the reactor was purged with He. Two different reaction mixtures were used for the catalytic tests (TG1, $CO{:}CO_2{:}H_2$ = 10:4:72, balanced in He, and TG2, $CO_2{:}H_2$ = 22:66, also balanced in He) using a total flow rate of 12 mL/min. A 60 mg portion of fresh catalyst from the same batch was used for each test. Two different batches were used to confirm the reproducibility of the results. Helium was used as an internal standard. The catalytic tests were performed consecutively at 1 bar and at 20 bar, at three different reaction temperatures (210, 240, 270 °C). The reaction products were analyzed online by a 7890B gas chromatograph (GC; Agilent Technologies, Inc.) equipped with two thermal conductivity detectors (TCD) and a flame ionizing detector (FID). All data points were acquired after a steady state was reached and are an average of at least five consecutive injections in the GC.

RESULTS AND DISCUSSION

Representative AFM images of $Cu_{0.5}Ni_{0.5}$ NPs supported on SiO_2/Si(111) acquired before and after the NAP-XPS measurements are shown in Figure 1. The corresponding size distribution histograms are shown in Figure S3 (SI). It is

DOI: 10.1021/acs.jpcc.8b09912
J. Phys. Chem. C 2019, 123, 8421−8428

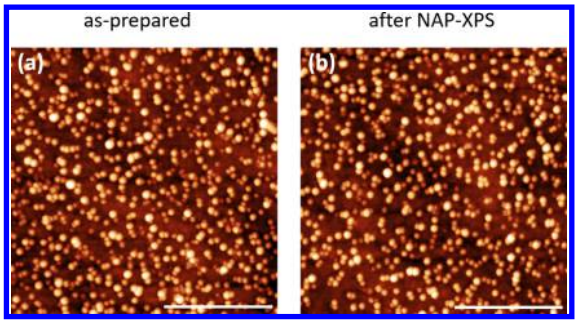

Figure 1. AFM images of size-selected (~5 nm) micellar CuNi NPs on SiO_2/Si(111) acquired at room temperature in air (a) after an *ex situ* O_2 plasma treatment and (b) after the NAP-XPS measurements, which were performed consecutively in O_2 (400 °C), in H_2 (400 °C), in a CO_2 + CO + H_2 (vol 4.5%:11.5%:84%) reaction mixture (210, 270 °C), again in O_2 (400 °C), and in pure CO (270 °C). The scale bars in the images correspond to 400 nm.

evident that the NPs do not undergo any significant morphological change during the NAP-XPS measurements. The average NP height and interparticle distance remain unaffected under NAP-XPS conditions, with no indication of sintering. This is at least partially assigned to the initial *ex situ* O_2 plasma treatment prior to the catalytic reaction that leads to the stabilization of the NPs on the substrate. Morphological characterization of the SiO_2-supported powder catalyst, performed by STEM/EDS before and after the catalytic reaction (Figure 2), confirms their bimetallic nature and the elemental composition of the NPs, as well as the absence of drastic agglomeration. An increase of the average NP size (up to 8 nm in some cases) was however observed after the reaction at 20 bar. Some local variations of the Cu:Ni metal ratio were observed from NP to NP in some cases, but the bimetallic nature of the NPs and the average elemental composition of $Cu_{0.5}Ni_{0.5}$ were confirmed in all investigated samples.

NAP-XPS spectra of the Cu $2p_{3/2}$ and Ni $2p_{3/2}$ core level regions acquired under different environmental conditions at two photon energies (1160 and 1540 eV) are shown in Figure 3.

Upon annealing in O_2 (0.4 mbar) at 400 °C, both metals are highly oxidized. Cu is present in the form of Cu^{2+} species, while the oxidation state of Ni is mostly Ni^{3+} (binding energy 856.8 eV), with only about 5% of NiO (855.1 eV) present. The presence of $Ni(OH)_2$ or NiO(OH) cannot be ruled out because the binding energy of these species is too close to that of Ni_2O_3 for a definite assignment. However, given that no source of hydrogen or water was present in the XPS chamber during the initial O_2 annealing, and in accordance with our previous studies of CuNi catalysts,[14] we tentatively attribute the peak at 856.8 eV to Ni_2O_3. Such species are unstable in bulk materials but have been reported for thin films and nanostructures.[18−20] They are created during the initial O_2 plasma treatment and have been shown to play an important role in determining the segregation trend in CuNi catalysts.[14] Another possibility that cannot be excluded is that the peak at 856.8 eV is due to Ni^{2+} species (NiO or mixed $Cu_xNi_{1-x}O$), with a spectral contribution shifted to higher binding energies due to nanoconfinement effects.

Subsequent treatment in H_2 (0.4 mbar, 400 °C) fully reduces both metals. The presence of Cu^+ species cannot be excluded, because the binding energies of Cu^0 and Cu^+ differ by only ~0.1 eV, and Cu LMM Auger lines, which would help distinguish between the two, could not be observed in our experiment due to the low NP coverage in our samples. However, given that Ni is fully reduced in H_2, it can be expected that Cu (which is more easily reduced) is mostly in its metallic state too. The oxidation state of the two metals remains unchanged under CO_2 hydrogenation reaction conditions in the gas mixture consisting of CO_2 + CO + H_2 (0.48 mbar; 210 and 270 °C). Subsequent annealing in O_2 (0.4 mbar, 400 °C) reoxidizes the metals (CuO, Ni^{3+}/$Ni(OH)_2$, small amounts of NiO), while dosing CO at 270 °C in the last step of the NAP-XPS sequence brings the metals back to their mostly metallic state, with only small amounts of Ni_2O_3 remaining. As expected, higher amounts of nickel oxides are observed in CO at the higher photon energy (12% Ni_2O_3 at

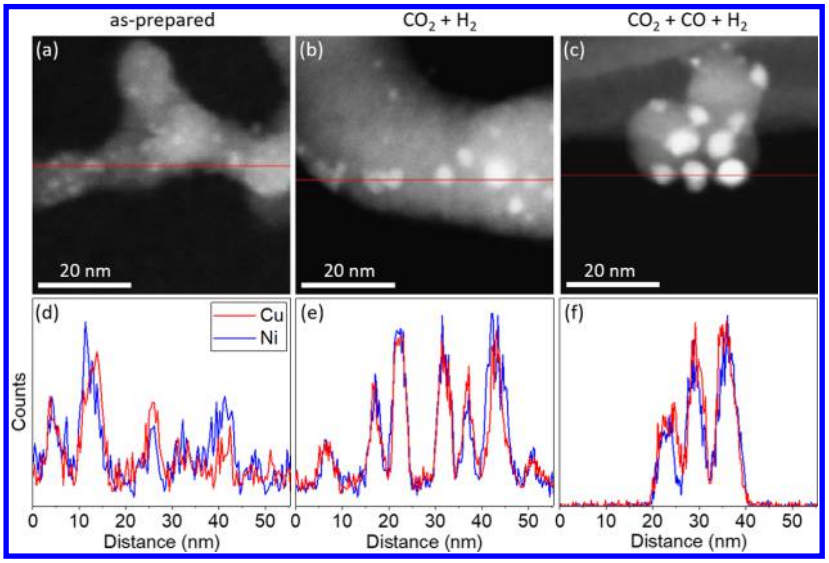

Figure 2. STEM images of a $Cu_{0.5}Ni_{0.5}/SiO_2$ powder catalyst obtained (a) before the catalytic reaction, (b) after catalytic reaction in CO_2 + H_2 (vol. 1:3) and (c) after catalytic reaction in CO_2 + CO + H_2 (vol. 4.5:11.5:84) at 20 bar (210−270 °C). EDS linear scans (d-f) show the relative amounts of Cu (red) and Ni (blue) along the lines shown in the respective STEM images in the upper row.

DOI: 10.1021/acs.jpcc.8b09912
J. Phys. Chem. C 2019, 123, 8421−8428

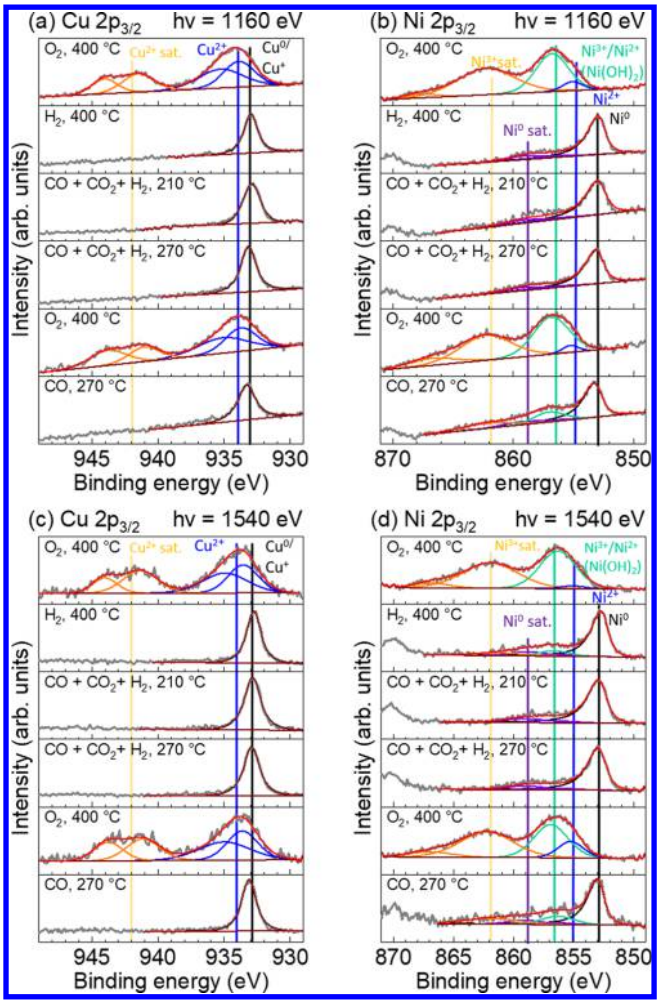

Figure 3. NAP-XPS spectra of the Cu $2p_{3/2}$ (a, c) and Ni $2p_{3/2}$ (b, d) core level regions of CuNi NPs on SiO_2/Si(111) acquired *in situ* in different gases (at a pressure of 0.4 mbar for the pure gases and 0.48 mbar for the reactant mixture) at the temperatures indicated on the graphs. X-ray photon energies of (a, b) 1160 eV and (c, d) 1540 eV were used for acquiring the depth profiles of the NPs.

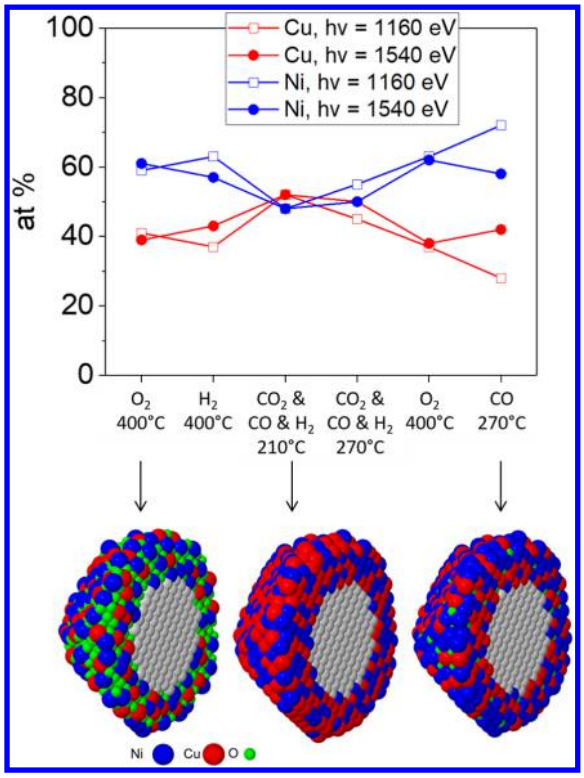

Figure 4. Cu (red) and Ni (blue) atomic percentages extracted from NAP-XPS measurements acquired *in situ* in the presence of various gases (at a pressure of 0.4 mbar for the pure gases and 0.48 mbar for the reactant mixture) at the indicated temperatures. The insets show cartoons displaying atomic models of the NPs depicting the variation of the elemental composition with the distance from the surface, as determined by NAP-XPS. The gray area in the center represents the volume of the NPs which is not probed in our XPS measurements (deeper than the IMFP in the accessible energy range). The model representations are for visual purposes only and do not reflect the actual crystallographic positions and sizes of the different atoms.

1540 eV) than at the surface-probing lower photon energy (9% Ni_2O_3 at 1160 eV), consistent with the fact that the reduction starts at the surface of the NPs and proceeds inward. The binding energies of the various Cu and Ni species, as determined from the fitting curves of the NAP-XPS spectra, are shown for the various environmental conditions in Figure S4 (SI).

The atomic percentages of the NPs at the two different probing depths were determined from the integrated intensities of the NAP-XPS peaks and summarized in Figure 4. After the initial O_2 annealing, the Ni:Cu atomic ratio is approximately equal to 60:40 at both photon energies. The fact that more Ni is probed in the near-surface volume of the NPs than what would be expected on the basis of the nominal atomic ratio indicates that surface segregation of Ni takes place when the NPs are fully oxidized. Subsequent reduction in H_2 results in a further increase of the amount of Ni directly at the surface (1160 eV) and a decrease deeper inside the NPs (1540 eV), while the opposite trend is observed for Cu. This indicates surface segregation of Ni in the presence of H_2.

Interestingly, the above trend is inverted upon heating in the reaction gas mixture consisting of CO_2 + CO + H_2 (vol 11.5:4.5:84). Already at a temperature of 210 °C, a significant increase of the Cu amount probed both at 1160 eV (increase from 37% to 53%) and at 1540 eV (increase from 45% to 53%) is observed, accompanied by a relative decrease of the Ni amount (from 63% to 47% at 1160 eV). These results clearly demonstrate surface segregation of Cu in the three-gas reaction mixture. At 270 °C, the Ni:Cu ratio on the surface slightly increases (to 55:45). Reoxidation of the NPs in O_2 after the reaction brings the particle composition back to its initial state, with Ni segregating again back to the surface (63% Ni at 1160 eV). The restructuring undergone by the NPs in the reactant mixture is thus fully reversible. The final step of the treatment sequence involves heating the sample in pure CO. As clearly shown in Figure 4, this induces strong Ni surface segregation, with a Ni:Cu ratio of 72:28 at 1160 eV (i.e., in the near-surface region) and 58:42 at 1540 eV (i.e., deeper into the NPs). The results of the NAP-XPS studies can be thus summarized as moderate surface segregation of Ni in O_2, stronger Ni surface segregation in H_2, and even stronger segregation in CO, with a remarkable inversion of this trend in a reaction mixture consisting of CO_2, CO, and H_2, which drives more Cu to the surface as compared to pure H_2 or CO, especially at the lower temperature (210 °C). A summary of the atomic percentages of the various metal species probed by NAP-XPS in all gaseous environments is given in Table S3 (SI).

DOI: 10.1021/acs.jpcc.8b09912
J. Phys. Chem. C 2019, 123, 8421−8428

The surface segregation of Cu observed in the CO-containing reaction mixture is surprising at first glance. Previous studies of the CuNi NPs have shown that annealing in a CO_2 + H_2 mixture (1:3 volume ratio) results in Ni surface segregation.[14] Given that annealing in pure CO also drives Ni to the surface (Figure 4), one might have expected the same result for the CO_2 + CO + H_2 environment too. In order to understand the reason for the unexpected surface segregation of Cu in the latter gas mixture, we performed density functional theory (DFT) calculations in a model system consisting of a Ni-doped Cu crystal with a (211) crystallographic surface orientation. The (211) surface is an approximation of the step edges that compose the surface of large NPs, as is the case here.[1,6,21] The segregation energy of a Ni solute atom in a Cu host lattice was calculated for various adsorbates (reactants, intermediate species, and final reaction products) at the surface of the system and for various Ni concentrations. The stability of the intermediate species was also calculated to provide an estimate of the relative significance of each adsorbate with respect to the determination of the segregation behavior. The calculated segregation energies along with the predicted segregation trends are shown in Table S4 (SI).

The segregation energy of Ni in a Cu host lattice with (211) surface is equal to −0.06 eV in O_2, −0.2 eV in H_2, and −0.46 eV in CO, indicating weak, moderate, and strong surface segregation of Ni, respectively, in these environments, in accordance with our NAP-XPS results. The calculations also indicate an energy value close to zero (−0.01 eV) for the segregation energy in a two-gas reactant mixture consisting of CO_2 and H_2. This is in accordance with previously reported NAP-XPS results which show that annealing in CO_2 + H_2 maintains the Ni surface segregation induced upon reduction in H_2[14]. The Ni segregation energy calculated for the three-gas reaction mixture CO_2 + CO + H_2 has a high negative value (−0.88 eV). This would mean stronger Ni surface segregation. The situation changes drastically, however, once the intermediate products formed during the main chemical reactions (methanation, methanol synthesis, reverse water gas shift reaction) are taken into consideration. These include HCOO, H_2COO(HCOOH), H_2COOH, H_2CO, H_3CO, and H_3COH.[22,23] A reliable identification of such intermediates directly from C 1s XPS spectra is very challenging, due to the large number of carbonaceous species with the same or very similar binding energy around 285−286 eV (see Figure S5, SI). $(CH)_x$ species are expected at binding energies around 284.7 eV and methoxy (CH_3O) species around 285.8 eV (see Table S5, Supporting Information). It is worth noting that the highest amount of carbonaceous adsorbates is measured under reaction conditions in CO_2 + CO + H_2 at 210 °C, i.e., under the conditions where the strongest Cu surface segregation was experimentally observed (Figure S6, Supporting Information).

Nickel tetracarbonyls ($Ni(CO)_4$) are common volatile species known to form when Ni comes in contact with CO.[24] The formation rate of these species is maximum at a temperature around 75−125 °C and drops sharply at higher temperatures.[25−27] Although formation of carbonyl species while ramping up the sample temperature in the CO-containing reactant mixture or in pure CO in our measurements is possible, no indication of such adsorbates could be seen in our Ni $2p_{3/2}$ XPS spectra at 210−270 °C in the binding energy region of 854.7−855.0 eV, where these would be expected.[28,29] Furthermore, no change of the Ni to Si atomic ratio was observed under reaction conditions after the initial reduction (Figure S7, Supporting Information), which is additional evidence that no significant loss of Ni through volatile $Ni(CO)_4$ species occurred during the NAP-XPS measurements. The fact that the same observation, i.e., no significant loss of Ni, is also made in the ICP-OES measurements (see Table S1, Supporting Information) and in the STEM/EDS characterization (Figure 2) of the silica-supported powder catalyst after reaction at a much higher pressure (20 bar) further supports this conclusion. Even if low concentrations of such adsorbates are present under reaction conditions in NAP-XPS, they are not expected to affect the segregation trend significantly, as discussed below.

The calculations (Figures S8−S10, Supporting Information) showed that, compared with other species formed under reaction conditions, such as HCOO, CH_2O, and $Ni(CO)_4$, CH_3O is more stable, thus dominating the segregation behavior. The reaction of coadsorbed H and CO to form CH_3O is exothermic by about 0.16 eV. The reaction energy for gas phase CO, H_2, and CO_2 to form adsorbed CH_3O species is −3.15 eV, while the reaction energies to form HCOO and CH_2O are −1.78 and −2.23 eV, respectively. Accordingly, CH_3O is the main species formed in the CO_2 + CO + H_2 mixture. This species is thus expected to dominate the segregation behavior experimentally observed. Once CH_3O is formed on the surface of the catalyst, the segregation energy of Ni changes sign from negative (−0.88 eV) to positive (+0.22 eV), indicating inward segregation of Ni and surface segregation of Cu. This result provides a viable explanation for the inversion of the segregation trend in the CO_2 + CO + H_2 reaction mixture which is observed in our NAP-XPS studies compared to the CO-free mixture. The CH_3O species is only formed in the three-gas mixture, when both H_2 and CO are present. It is expected that increasing the reaction temperature from 210 to 270 °C accelerates the decomposition of the species (due to the higher entropy), thus limiting the Cu surface segregation trend. The $Ni(CO)_4$ species, if present, are not significant for the observed segregation behavior because they are very unstable: our stability calculations show that, after relaxation, $Ni(CO)_4$ changes to four CO molecules adsorbed on the surface. The fact that the experimentally observed segregation behavior (Figure 4) in the CO-containing reactant mixture is very different from that in pure CO (where a higher concentration of $Ni(CO)_4$ should be expected) further supports the conclusion that Ni carbonyls do not play a significant role in the segregation phenomena in our measurements under reaction conditions. It is noted that the HCOO species which are formed in the CO-free reactant mixture in principle also induces minimal surface segregation of Cu (segregation energy of 0.03 eV), but the lower stability of this species and the nearly zero segregation energy value mean that its presence is barely sufficient to invert the surface segregation of Ni observed in the CO_2 + H_2 mixture upon reduction in H_2.[14]

For the catalytic characterization of the silica-supported CuNi NPs in the fixed-bed reactor, the same reactant mixture and temperatures as in the NAP-XPS measurements, but higher pressures (1 and 20 bar versus 0.48 mbar for the NAP-XPS), were used. The catalyst was found to be highly selective toward methanol (86%) in CO_2 + CO + H_2 at 20 bar at a temperature of 210 °C (Figure 5a). The low-pressure and -temperature conditions under which such high selectivity is achieved make the catalyst an attractive alternative to the

DOI: 10.1021/acs.jpcc.8b09912
J. Phys. Chem. C 2019, 123, 8421−8428

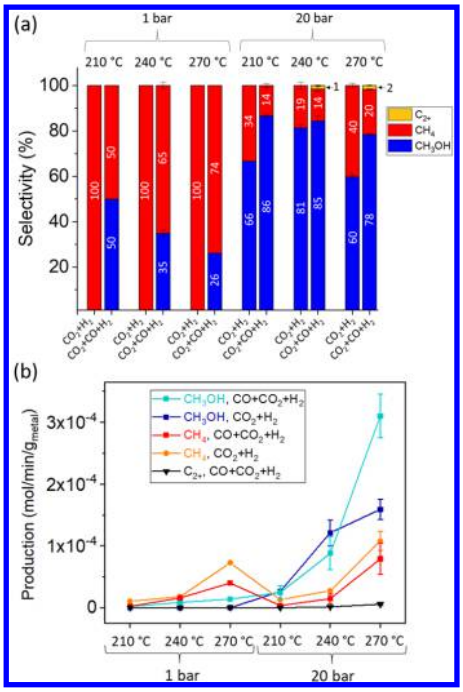

Figure 5. (a) Selectivity toward methanol, methane, and C_2/C_3 products (ethane, propylene) during CO_2 hydrogenation over the CuNi/SiO_2 powder catalyst measured in a fixed-bed flow reactor in two different CO_2 hydrogenation reactant mixtures (with and without CO) at two different pressures (1 and 20 bar). CO is not included as a product. (b) Production rate of methanol, methane, and C_2/C_3 products (ethane, propylene) during the catalytic testing of the CuNi/SiO_2 catalyst. The normalization was based on the total metal (Cu + Ni) content (in milligrams) as determined by ICP-OES (Table S1, Supporting Information). The error bars, both in parts a and b, indicate standard deviation errors (repetition of characterization on different, identically synthesized catalyst samples).

industrial catalyst. Furthermore, the methanol promoting effect of CO in the reactant mixture is significant already at atmospheric pressure, where 50% methanol selectivity is achieved at 210 °C in CO_2 + CO + H_2, whereas only CH_4 is produced under the same conditions in CO_2 + H_2 (Figure 5a). The methanol promoting effect is also obvious in the catalytic activity of the system: the methanol production rate at 20 bar and 270 °C is about 2 times higher in the CO_2 + CO + H_2 mixture than in CO_2 + H_2 (Figure 5b). The value of 3.1 × 10^{-4} mol/min/g we have found for the methanol production rate under these conditions is higher by a factor of ∼3.2 than the maximum rate previously reported for a Cu_xNi_y/γ-Al_2O_3 catalyst at 290 °C.[3] Although the large pressure difference (by more than 4 orders of magnitude) between the NAP-XPS measurements (0.48 mbar) and the catalytic characterization (lowest pressure: 1 bar) makes a direct comparison of the results difficult, it is noteworthy that the NPs used in the NAP-XPS measurements are highly active when supported on silica even at moderate pressure, clearly demonstrating the methanol promotion effect resulting from the presence of CO in the reactant mixture.

Our results are of significance for understanding the effect that the presence of Ni on the surface of Cu-based catalysts and of CO in the reactant mixture has on the methanol synthesis efficiency during CO_2 hydrogenation. The assumption made in previous literature reports that the addition of CO to the reactant mixture promotes methanol synthesis due to the induced surface segregation of Ni is not supported either by our experimental or by our theoretical results.[2,10] In contrast, our study indicates that the presence of CO in the reactant mixture actually causes Cu surface segregation due to the formation of the stable intermediate species CH_3O. While direct experimental determination of the produced intermediates under catalytic reaction conditions was not unambiguously feasible in our NAP-XPS study, our calculations demonstrate that the formation of CH_3O is the only factor that is different in the CO_2 + CO + H_2 experiment as compared to the one performed in the CO-free reactant mixture. The fact that CH_3O is an important intermediate during CO hydrogenation over Cu-based catalysts has been previously established in the literature.[1,6] Given that all other factors affecting the segregation behavior are identical in the two environments, and following the theoretical findings presented, it is plausible to conclude that the role of reaction intermediates should be taken into consideration when searching for the reasons for the enhanced methanol synthesis obtained for CuNi NPs in CO_2 + CO + H_2 mixtures. CH_3O can be easily hydrogenated to methanol; thus, it is reasonable to expect that the formation of this intermediate is beneficial for methanol formation. When no CO is present in the reactant feed, very limited amounts of this intermediate are formed (only those originating from the CO which is produced from CO_2 via reverse water gas shift reaction). The methanation of CO_2 through the Sabatier reaction is then favored. The rather unexpected surface segregation of Cu under reaction conditions in the CO_2 + CO + H_2 reactant mixture should be kept in mind when determining the initial elemental surface composition of the catalytic system, so that the desired copper to nickel atomic ratio is eventually achieved upon surface restructuring during the reaction.

■ CONCLUSIONS

Near-ambient pressure XPS measurements, performed at moderate temperatures in various gas environments, in combination with DFT calculations, revealed the elemental composition of bimetallic CuNi NPs in the presence of different surface adsorbates. We demonstrated that copper surface segregation takes place under CO_2 hydrogenation reaction conditions in a three-gas mixture consisting of CO_2, CO, and H_2. This is in contrast to previously reported observations of Ni surface segregation in a CO-free gas mixture (CO_2 + H_2), as well as to the strong surface segregation of Ni reported here in a pure CO environment. On the basis of our DFT calculations, this segregation trend could be assigned to the formation of a stable intermediate species (CH_3O) in CO_2 + CO + H_2, which changes the sign of the segregation energy of Ni from negative to positive, thus inducing outward segregation of Cu.

Moreover, analogously synthesized CuNi NPs supported on nanocrystalline SiO_2 were found to exhibit high catalytic activity and selectivity (up to 86%) toward methanol at moderate pressures and temperatures (20 bar, 210−270 °C). Our results shed new light on the factors determining the methanol synthesis efficiency of CuNi catalysts, disqualifying the previously assumed CO-induced surface segregation of Ni in the three-gas mixture, and underlining the crucial role of intermediate reaction products as driving forces of segregation phenomena. It is evident that knowing which reaction intermediates are stable under reaction conditions is key for

DOI: 10.1021/acs.jpcc.8b09912
J. Phys. Chem. C 2019, 123, 8421−8428

identifying the adsorbate effect that will dominate the segregation trend during the reaction.

■ ASSOCIATED CONTENT

Supporting Information

The Supporting Information is available free of charge on the ACS Publications website at DOI: 10.1021/acs.jpcc.8b09912.

Details on XPS analysis, catalyst synthesis, and theoretical calculations; histograms of NP heights from AFM; binding energies and atomic ratios of metal species; calculated segregation energies from DFT; C 1s XPS spectra; structural and energetic information used in the DFT calculations; IMFP of photoelectrons; and ICP-OES results (PDF)

■ AUTHOR INFORMATION

Corresponding Author

*E-mail: Roldan@fhi-berlin.mpg.de.

ORCID

Ioannis Zegkinoglou: 0000-0002-1101-6935

Carlos Escudero: 0000-0001-8716-9391

Beien Zhu: 0000-0002-0126-0854

Yi Gao: 0000-0001-6015-5694

Beatriz Roldan Cuenya: 0000-0002-8025-307X

Notes

The authors declare no competing financial interest.

■ ACKNOWLEDGMENTS

We thank Dr. Olaf Timpe (FHI) for the ICP-OES measurements. This work was funded by the European Research Council under Grant ERC-OPERANDOCAT (ERC-725915). The TEM work was supported by the Cluster of Excellence RESOLV at RUB (EXC 1069) funded by the Deutsche Forschungsgemeinschaft (DFG). C.E. acknowledges financial support from the Spanish government (MAT2012-38567-C02-02).

■ REFERENCES

(1) Behrens, M.; Studt, F.; Kasatkin, I.; Kühl, S.; Hävecker, M.; Abild-Pedersen, F.; Zander, S.; Girgsdies, F.; Kurr, P.; Kniep, B. L.; et al. The Active Site of Methanol Synthesis over $Cu/ZnO/Al_2O_3$ Industrial Catalysts. *Science* **2012**, *336*, 893−897.

(2) Nerlov, J.; Chorkendorff, I. Methanol Synthesis from CO_2, CO, and H_2 over Cu(100) and Ni/Cu(100). *J. Catal.* **1999**, *181*, 271−279.

(3) Zhao, F.; Gong, M.; Zhang, Y.; Li, J. The Performance and Structural Study of CuNi Alloy Catalysts for Methanol Synthesis. *J. Porous Mater.* **2016**, *23*, 733−740.

(4) Zhao, F.; Gong, M.; Cao, K.; Zhang, Y.; Li, J.; Chen, R. Atomic Layer Deposition of Ni on Cu Nanoparticles for Methanol Synthesis from CO_2 Hydrogenation. *ChemCatChem* **2017**, *9*, 3772−3778.

(5) Yang, Y.; White, M. G.; Liu, P. Theoretical Study of Methanol Synthesis from CO_2 Hydrogenation on Metal-Doped Cu(111) Surfaces. *J. Phys. Chem. C* **2012**, *116*, 248−256.

(6) Studt, F.; Abild-Pedersen, F.; Wu, Q.; Jensen, A. D.; Temel, B.; Grunwaldt, J.-D.; Nørskov, J. K. CO Hydrogenation to Methanol on Cu−Ni Catalysts: Theory and Experiment. *J. Catal.* **2012**, *293*, 51−60.

(7) Vesselli, E.; Monachino, E.; Rizzi, M.; Furlan, S.; Duan, X.; Dri, C.; Peronio, A.; Africh, C.; Lacovig, P.; Baldereschi, A.; et al. Steering the Chemistry of Carbon Oxides on a NiCu Catalyst. *ACS Catal.* **2013**, *3*, 1555−1559.

(8) Chinchen, G. C.; Denny, P. J.; Parker, D. G.; Spencer, M. S.; Whan, D. A. Mechanism of Methanol Synthesis from $CO_2/CO/H_2$ Mixtures over Copper/Zinc Oxide/Alumina Catalysts - Use of ^{14}C-Labeled Reactants. *Appl. Catal.* **1987**, *30*, 333−338.

(9) Yang, Y.; Mims, C. A.; Mei, D. H.; Peden, C. H. F.; Campbell, C. T. Mechanistic Studies of Methanol Synthesis over Cu from $CO/CO_2/H_2/H_2O$ Mixtures: The Source of C in Methanol and the Role of Water. *J. Catal.* **2013**, *298*, 10−17.

(10) Nerlov, J.; Chorkendorff, I. Promotion through Gas Phase Induced Surface Segregation: Methanol Synthesis from CO, CO_2 and H_2 over Ni/Cu(100). *Catal. Lett.* **1998**, *54*, 171−176.

(11) Yao, Y.; Goodman, D. W. In Situ IR Spectroscopic Studies of Ni Surface Segregation Induced by CO Adsorption on $Cu-Ni/SiO_2$ Bimetallic Catalysts. *Phys. Chem. Chem. Phys.* **2014**, *16*, 3823−3829.

(12) Roldan Cuenya, B.; Behafarid, F. Nanocatalysis: Size- and Shape-Dependent Chemisorption and Catalytic Reactivity. *Surf. Sci. Rep.* **2015**, *70*, 135−187.

(13) Pérez-Dieste, V.; Aballe, L.; Ferrer, S.; Nicolàs, J.; Escudero, C.; Milán, A.; Pellegrin, E. Near Ambient Pressure XPS at ALBA. *J. Phys.: Conf. Ser.* **2013**, *425*, 072023.

(14) Pielsticker, L.; Zegkinoglou, I.; Divins, N. J.; Mistry, H.; Chen, Y.-T.; Kostka, A.; Boscoboinik, J. A.; Roldan Cuenya, B. Segregation Phenomena in Size-Selected Bimetallic CuNi Nanoparticle Catalysts. *J. Phys. Chem. B* **2018**, *122*, 919−926.

(15) Blöchl, P. E. Projector Augmented-Wave Method. *Phys. Rev. B: Condens. Matter Mater. Phys.* **1994**, *50*, 17953−17979.

(16) Kresse, G.; Furthmüller, J. Efficient Iterative Schemes for Ab Initio Total-Energy Calculations Using a Plane-Wave Basis Set. *Phys. Rev. B: Condens. Matter Mater. Phys.* **1996**, *54*, 11169−11186.

(17) Kresse, G.; Furthmüller, J. Efficiency of Ab-Initio Total Energy Calculations for Metals and Semiconductors Using a Plane-Wave Basis Set. *Comput. Mater. Sci.* **1996**, *6*, 15−50.

(18) Wang, Z.; You, Y.; Yuan, J.; Yin, Y.-X.; Li, Y.-T.; Xin, S.; Zhang, D. Nickel-Doped $La_{0.8}Sr_{0.2}Mn_{1-x}Ni_xO_3$ Nanoparticles Containing Abundant Oxygen Vacancies as an Optimized Bifunctional Catalyst for Oxygen Cathode in Rechargeable Lithium−Air Batteries. *ACS Appl. Mater. Interfaces* **2016**, *8*, 6520−6528.

(19) Aggarwal, P. S.; Goswami, A. An Oxide of Tervalent Nickel. *J. Phys. Chem.* **1961**, *65*, 2105−2105.

(20) Kang, J.-K.; Rhee, S.-W. Chemical Vapor Deposition of Nickel Oxide Films from $Ni(C_5H_5)_2/O_2$. *Thin Solid Films* **2001**, *391*, 57−61.

(21) Zhang, X.; Liu, J.-X.; Zijlstra, B.; Filot, I. A. W.; Zhou, Z.; Sun, S.; Hensen, E. J. M. Optimum Cu Nanoparticle Catalysts for CO_2 Hydrogenation Towards Methanol. *Nano Energy* **2018**, *43*, 200−209.

(22) Wu, H. C.; Chang, Y. C.; Wu, J. H.; Lin, J. H.; Lin, I. K.; Chen, C. S. Methanation of CO_2 and Reverse Water Gas Shift Reactions on Ni/SiO_2 Catalysts: The Influence of Particle Size on Selectivity and Reaction Pathway. *Catal. Sci. Technol.* **2015**, *5*, 4154−4163.

(23) Liu, Y.-M.; Liu, J.-T.; Liu, S.-Z.; Li, J.; Gao, Z.-H.; Zuo, Z.-J.; Huang, W. Reaction Mechanisms of Methanol Synthesis from CO/CO_2 Hydrogenation on $Cu_2O(111)$: Comparison with Cu(111). *J. CO_2 Util.* **2017**, *20*, 59−65.

(24) Mihaylov, M.; Hadjiivanov, K.; Knözinger, H. Formation of $Ni(CO)_4$ During the Interaction between CO and Silica-Supported Nickel Catalyst: An FTIR Spectroscopic Study. *Catal. Lett.* **2001**, *76*, 59−63.

(25) Shen, W. M.; Dumesic, J. A.; Hill, C. G. Criteria for Stable Ni Particle Size under Methanation Reaction Conditions: Nickel Transport and Particle Size Growth Via Nickel Carbonyl. *J. Catal.* **1981**, *68*, 152−165.

(26) De Groot, P.; Coulon, M.; Dransfeld, K. $Ni(CO)_4$ Formation on Single Ni Crystals: Reaction Kinetics and Observation of Surface Facetting Induced by the Reaction. *Surf. Sci.* **1980**, *94*, 204−220.

(27) Liang, D. B.; Abend, G.; Block, J. H.; Kruse, N. Formation of Nickel Subcarbonyls from Nickel and Carbon Monoxide. *Surf. Sci.* **1983**, *126*, 392−396.

(28) Czekaj, I.; Loviat, F.; Raimondi, F.; Wambach, J.; Biollaz, S.; Wokaun, A. Characterization of Surface Processes at the Ni-Based Catalyst During the Methanation of Biomass-Derived Synthesis Gas: X-Ray Photoelectron Spectroscopy (XPS). *Appl. Catal., A* **2007**, *329*, 68−78.

(29) Matienzo, J.; Yin, L. I.; Grim, S. O.; Swartz, W. E. X-Ray Photoelectron Spectroscopy of Nickel Compounds. *Inorg. Chem.* **1973**, *12*, 2762−2769.

DOI: 10.1021/acs.jpcc.8b09912
J. Phys. Chem. C 2019, 123, 8421−8428